https://doi.org/10.5194/gmd-2021-11
Preprint. Discussion started: 8 March 2021

Geoscientific Model Development Discussions
Open Access
EGU

Cloud Feedbacks from CanESM2 to CanESM5.0 and their Influence on Climate Sensitivity

John, G. Virgin[1], Christopher, G. Fletcher[1], Jason, N. S. Cole[2], Knut von Salzen[2], and Toni Mitovski[2,3]

[1]Department of Geography & Environmental Management, University of Waterloo, Waterloo, Ontario, Canada
[2]Canadian Centre for Climate Modelling and Analysis, Environment and Climate Change Canada, Victoria, British Columbia, Canada
[3]Ministry of Health, Government of British Columbia, Victoria, British Columbia, Canada

Correspondence: John G. Virgin (jgvirgin@uwaterloo.ca)

Abstract.

The newest iteration of the Canadian Earth System Model (CanESM5.0.3) has an Effective Climate Sensitivity (ECS) of 5.65 kelvin, which is a 54% increase relative to the model's previous version (CanESM2 - 3.67 K), and the highest sensitivity of all current models participating in the sixth phase of the coupled model inter-comparison project (CMIP6). Here, we explore the underlying causes behind CanESM5's increased ECS via comparison of forcing and feedbacks between CanESM2 and CanESM5. We find only modest differences in radiative forcing as a response to CO_2 between model versions. Through the use of cloud area fraction output and radiative kernels, we find that more positive shortwave cloud feedbacks— particularly with regards to low clouds across the equatorial pacific, as well as sub/extratropical free troposphere cloud optical depth— are the dominant contributors to CanESM5's increased climate sensitivity. Additional simulations with prescribed sea surface temperatures reveal that the spatial pattern of surface temperature change explains the pattern of change in low cloud fraction, but does not fully explain the increased ECS in CanESM5. The results from CanESM5 are consistent with increased ECS in several other CMIP6 models, which has been primarily attributed to changes in shortwave cloud feedbacks.

1 Introduction

Equilibrium Climate Sensitivity (ECS), defined as the global, annual mean surface warming the Earth would exhibit as a response to a doubling of CO_2, is a frequently cited emergent property for Earth system models (Andrews et al., 2012; Vial et al., 2013; Charney et al., 1979). The first estimates of ECS from Earth system models ranged from 1.5 - 4.5 K (Charney et al., 1979). In the latest phase of the Coupled Model Inter-comparison Project (CMIP6), the range of ECS from participating models has widened (1.8 - 5.5 K), with the mean shifting towards higher values than the previous phase of CMIP (3.2 to 3.7 K from CMIP5 to CMIP6) (Flynn and Mauritsen, 2020; Zelinka et al., 2020). Inter-model spread of ECS is primarily attributed

https://doi.org/10.5194/gmd-2021-11
Preprint. Discussion started: 8 March 2021


Geoscientific Model Development Discussions

to radiative feedbacks on the climate system- specifically with regards to cloud feedbacks, which are the primary source of spread across models (Caldwell et al., 2016; Vial et al., 2013; Dufresne and Bony, 2008).

Understanding cloud feedback uncertainty and its influence on the ECS of Earth system models (ESMs) has been an imperative of researchers in recent decades- particularly with regards to properties such as cloud optical depth, which reflect shortwave (SW) radiation and cool the planet (Vial et al., 2013; Tan et al., 2016; Zelinka et al., 2020; Bjordal et al., 2020). SW cloud feedbacks can be separated based on latitude; middle latitude SW cloud feedbacks are mostly negative from the optical thickening of clouds due to phase transition towards liquid in ice/mixed phase clouds (Goosse et al., 2018; Senior and Ingram, 1989). In high latitudes, sea ice loss exposes the ocean surface and increases surface turbulent fluxes, and therefore humidity, which increases low level cloudiness (Goosse et al., 2018). In low latitudes, the SW cloud feedback is robustly positive in both ESMs and Large Eddy Simulations (LES), owing to a reduction in the fraction and thickness of marine shallow cumulus and stratocumulus clouds near the planetary boundary layer (PBL) (Bretherton and Blossey, 2014; Bretherton et al., 2013; Ceppi et al., 2017). The physical mechanisms behind SW low cloud feedbacks are tied to multiple thermodynamic, radiative, and dynamical processes- termed cloud controlling factors (CCFs) (Klein et al., 2017). Specifically, mechanisms favoring an increase in low cloud fraction in baseline climatology regimes include stronger PBL temperature inversions (Wood and Bretherton, 2006; Klein and Hartmann, 1993; Bretherton et al., 2013), colder sea surface temperatures (SST) (Bretherton and Blossey, 2014), less subsidence (Blossey et al., 2013), and increased free troposphere humidity (Van der Dussen et al., 2015).

While the sensitivity of marine low cloud cover (LCC) to specific factors varies significantly from model to model, differing sensitivities to SSTs have been identified as a explanatory factor for spread across ESMs (Qu et al., 2014). This link suggests the spatial pattern of surface warming has important implications for low cloud responses (Rose et al., 2014; Zhou et al., 2015), and therefore the SW cloud feedback and climate sensitivity (Andrews and Webb, 2018).

Here, we investigate the causes of increased climate sensitivity in the newest version of the Canadian Earth System Model, which is the highest of all models currently participating in CMIP6, relative to the previous model version that was contributed to CMIP5 (CanESM2). (Flynn and Mauritsen, 2020). With a particular focus on decomposed cloud feedbacks, we quantify the differences in both forcing and feedback between CanESM2 and CanESM5 in order to establish a physical link for the shift in ECS. Lastly, we examine the spatial pattern of warming in CanESM5 and its influence of both global mean and local cloud feedbacks as a potential explanatory variable for CanESM5's high ECS.

2 Methods

2.1 Models

We compare two versions of CanESM in this study. CanESM2, the second generation earth system model from the Canadian Centre for Climate Modelling and Analysis (CCCma), consists of their fourth generation atmosphere model (CanAM4), terrestrial carbon model (CTEM), CSM ocean model from the National Centre for Atmosphere Research (NCAR), and ocean carbon model (CMOC) (von Salzen et al., 2013; Arora et al., 2009; Zahariev et al., 2008; Arora et al., 2011; Gent et al., 1998). CanESM5, the newest generation of the Canadian Earth System Model, includes an updated version of the Canadian atmo-

https://doi.org/10.5194/gmd-2021-11
Preprint. Discussion started: 8 March 2021


Geoscientific Model Development Discussions

sphere model (CanAM5) and the land surface scheme, as well as brand new ocean and sea ice models. For a full review of the components in CanESM5, see Swart et al. (2019).

2.2 Forcing-Feedback Analysis

We consider energy balance at Earth's top of atmosphere (TOA) using the following equation:

$$N = F - \lambda \Delta T_s \tag{1}$$

Where N is net radiation imbalance (in Wm^{-2}), F is the Effective Radiative Forcing (ERF) due to that of an external agent (e.g. CO_2, in Wm^{-2}), ΔT_s is the global, annual mean surface temperature response (in Kelvin), and λ is the net Climate Feedback Parameter (CFP, in $Wm^{-2}K^{-1}$). Equation 1 assumes a linear relationship between radiation imbalance and surface temperature response (i.e. a constant λ). Under this assumption, an earth system model with a stronger (more negative) λ term will reestablish energy balance faster- and with a weaker surface temperature response- than a weak λ term. We calculate the CFP using pre-industrial control and abrupt-4xCO_2 experiments for each version of CanESM. For CanESM2, we use 150 years of pre-industrial control and abrupt 4xCO_2 coupled model output submitted to to the Earth System Grid Federation under run 1, initialization 1, and physics 1 (r1i1p1) (Taylor et al., 2012). For CanESM5, we use the same experiments submitted for the core CMIP6 experiment deck (Eyring et al., 2016).

The surface temperature response after the system has reached equilibrium ($N = 0$ Wm^{-2}) is defined as the Equilibrium Climate Sensitivity, which is typically measured under a 2xCO_2 ERF ($ECS = -F/\lambda$). We use the term "Effective", as opposed to "Equilibrium" Climate Sensitivity given the linear assumptions in Equation 1, where Equilibrium Climate Sensitivity takes into account a time varying CFP and is representative of warming once the system as reached true equilibrium (Knutti et al., 2017). The extent that the linear approximation accurately represents both forcing and feedback varies from model to model, where some models exhibit a more linear response to CO_2 than others (Andrews et al., 2012). The time varying CFP has been- at least in part- attributable to differences in model timescale and magnitude of "rapid adjustments" in the climate system, where quick tropospheric climate response to CO_2 modifies TOA energy balance (Smith et al., 2018; Forster et al., 2013; Sherwood et al., 2015).

We consider the influence of rapid adjustments by diagnosing the ERF using two distinct methods. First, we use an ordinary least squares linear regression between TOA radiation imbalance (N) and surface temperature response (ΔT_s) in abrupt 4xCO_2 experiments, where the extrapolated y-intercept of the regression line equals 2x the ERF (ERF_g, Gregory et al. (2004)). Second, we use 30 year fixed sea surface temperature (sstClim) experiments (piControl and abrupt 4xCO_2) submitted to the Radiative Forcing Model Inter-comparison Project (RFMIP) (Pincus et al., 2016). The ERF is calculated by differencing net TOA radiation in 30 year annual mean fixed sea surface temperature experiments (ERF_h), where one experiment uses pre-industrial control CO_2 and the other uses abrupt 4xCO_2 (Hansen et al., 2005; Pincus et al., 2016). Under the ERF_h definition, both tropospheric and stratospheric rapid adjustments from clouds, air temperature, water vapour, and surface albedo are included along with CO_2.

https://doi.org/10.5194/gmd-2021-11
Preprint. Discussion started: 8 March 2021


Geoscientific Model Development Discussions

Using the Gregory regression method, we obtain the CFP as the slope of the regression line. Furthermore, we quantify the ECS for an abrupt 2xCO_2 forcing as the extrapolated x-intercept of the regression line divided by two. We consider the CFP as the linear sum of individual radiative feedbacks within the climate system:

$$\lambda = \lambda_p + \lambda_{lr} + \lambda_{wv} + \lambda_a + \lambda_c + R_e \tag{2}$$

Where the CFP is made up of contributions from the Planck (λ_p), lapse rate (λ_{lr}), water vapour (λ_{wv}), surface albedo (λ_a), and cloud (λ_c) feedbacks. A residual term is also included (R_e) in order to account for nonlinearities. We use a combination of the radiative kernel and Gregory regression methods to diagnose individual radiative feedbacks (Block and Mauritsen, 2013; Soden and Held, 2006). Specifically, we use six sets of radiative kernels to calculate TOA fluxes for temperature, water vapour, and surface albedo responses (Soden et al., 2008; Block and Mauritsen, 2013; Shell et al., 2008; Pendergrass et al., 2018; Huang et al., 2017; Smith, 2018). Then, each flux is linearly regressed against global, annual mean surface temperature response for 150 years, where the slope of the regression line is considered the feedback value (in $Wm^{-2}K^{-1}$). We use the clear sky linearity test to validate the accuracy of each radiative kernel (Shell et al., 2008), where the sum of all clear sky feedbacks is compared against the net clear sky climate feedback parameter as estimated using the Gregory regression technique with clear sky TOA flux. Three radiative kernels passed the clear sky linearity test (relative errors of less than 10%) (Figure A1), which are used to calculate an ensemble kernel mean for all feedbacks.

2.3 Cloud Feedbacks

Cloud feedbacks cannot be calculated via the standard radiative kernel method due to nonlinearities associated with cloud vertical overlap (Soden et al., 2008). We estimate cloud feedbacks using two methods- the adjusted Cloud Radiative Effect (CRE) and cloud radiative kernel method. The CRE response is defined as the difference between clear and total sky radiative fluxes. We adjust the CRE for the effects of environmental masking from other feedbacks using clear sky radiative kernels (Soden et al., 2004). The CRE 'adjustment' using clear sky radiative kernels takes into account differences in temperature and water vapour between a clear and cloudy atmosphere to isolate the radiative perturbation from clouds. We also account for the masking effect of CO_2 forcing by using a globally uniform proportionality constant between clear and total sky CO_2 forcing (Soden et al., 2008; Chung and Soden, 2015). After adjusting the CRE, the cloud flux response is regressed similarly to noncloud feedbacks, where the slope of the regression line equals the cloud feedback. This method is performed twice to yield a value for both the shortwave (SW) and longwave (LW) cloud feedbacks.

We use cloud radiative kernels and cloud area fraction output from the International Satellite Cloud Climatology Project (ISCCP), produced from the CFMIP Observation Simulator Package (COSP) (Bodas-Salcedo et al., 2011) in CanESM2 and CanESM5, to diagnose cloud feedbacks for different cloud top pressures and optical depths (Zelinka et al., 2012a). Specifically, we calculate a cloud area fraction response, relative to a pre-industrial control climatology, for every year, grid point, optical depth, and cloud top pressure bin for each year in the abrupt 4xCO_2 simulation. Then, cloud radiative kernels are applied to the cloud area fraction response to derive TOA flux perturbations. Similar to noncloud feedbacks, each point is then linearly

https://doi.org/10.5194/gmd-2021-11
Preprint. Discussion started: 8 March 2021


Geoscientific Model Development Discussions

regressed against global, annual mean surface temperature response over 150 years, where the slope of the regression line is equal to the feedback value.

In this study, we consider low clouds as having their tops $\geq$ 680 hPa and non-low clouds with tops $\leq$ 680 hPa. A key limitation of COSP output is the potential obscuring of low clouds via shift in the distribution of high cloud fraction (Zelinka et al., 2018). We account for the obscuring of low clouds via normalizing low cloud fraction by upper level clear-sky fraction as in Scott et al. (2020). Using this method, non-obscured low cloud responses are weighted by the area fraction not covered by high clouds.

To further separate cloud feedbacks into contributions from cloud altitude, optical depth, and amount components, we utilize the refined decomposition technique as in Zelinka et al. (2016). Using this method, cloud kernels are decomposed into individual components for cloud amount, optical depth, altitude, and residuals, while cloud area fraction anomalies are resolved into contributions from altitude/optical depth shifts and total amount separately. For a full mathematical breakdown of this decomposition, see Appendix B in Zelinka et al. (2013) and the supplemental information document from Zelinka et al. (2016).

For CanESM2, only 40 years of cloud area fraction data (years 1-20 & 120-140) were available in the abrupt-4xCO_2 simulation. To test the impact of sample size on our results, we subsample the output from the CanESM5 abrupt-4xCO2 simulation for the same time periods as are available from CanESM2 (years 1-20 & 120-140) and find highly similar results to those obtained from the full 150 years (Figure A3). Furthermore, we find very similar results for LW and SW cloud feedback components from CanESM2 and CanESM5 computed using the radiative kernel method and the adjusted-CRE method (Figure A2). This provides confidence that both methods are accurately capturing the pattern and magnitude of cloud feedbacks in these models.

3 Results

3.1 Effective Climate Sensitivity & Radiative Forcing

We begin by quantifying net feedback, forcing, and ECS for CanESM2 and CanESM5 (Figure 1a). CanESM2 exhibits a total climate feedback parameter of -1.03 $Wm^{-2}K^{-1}$, with an ECS of 3.67 K (Figure 1a). Relative to CanESM2, CanESM5 has a weaker CFP (-0.64 $Wm^{-2}K^{-1}$) and higher ECS (5.65 K). From version 2 to 5, ECS has increased by 54%. For comparison, we also show the model range of ECS for both CMIP5 and 6 using horizontal lines below the x-axis in Figure 1a, illustrating the high ECS in CanESM5 relative to all other CMIP6 models (Flynn and Mauritsen, 2020). Despite the increased ECS in CanESM5, both versions of CanESM exhibit a strong linear relationship between surface temperature and net TOA flux. Correlation coefficients are 0.92 and 0.95 for CanESM2 and CanESM5, respectively. We now turn to the different components of the forcing-feedback framework to elucidate any changes in either forcing, or feedback, and their influence on ECS.

We compare the ERF for CanESM2 and CanESM5 via two methods. The ERF_g is determined by the y-intercept of the Gregory regression plots (filled in circles on the y-axis in Figure 1a). The ERF_g is 7.21 and 7.54 Wm^{-2} for CanESM2 and 5, respectively. For comparison, we also show the ERF_h as estimated using fixed-SST simulations submitted to RFMIP (open squares). Both versions of CanESM have comparable differences between ERF_h and ERF_g, ranging 3-5%. Given the ERF

https://doi.org/10.5194/gmd-2021-11
Preprint. Discussion started: 8 March 2021

Geoscientific Model Development Discussions

differences between both versions of CanESM cannot account for the ECS increase in CanESM5, the conclusion is that the change in ECS is related to feedbacks, rather than forcing. We next decompose the CFP for both models to elucidate the any potential differences in the strength of radiative feedbacks.

3.2 Radiative Feedbacks

Planck, lapse rate, water vapour, surface albedo, and cloud TOA feedbacks are shown in Figure 1b. Planck and lapse rate plus water vapour feedbacks are roughly equal between CanESM2 and CanESM5. The surface albedo feedback is more positive in CanESM5, showing an increase of 0.05 $Wm^{-2}K^{-1}$ over CanESM2, which is primarily due to increases over the Arctic from sea ice loss (Swart et al., 2019). Lastly, the cloud feedback is significantly stronger in CanESM5, with an increase over CanESM2 of 65%. The net feedback (sum of all individual feedbacks) is also shown in Figure 1b to demonstrate the strong agreement the sum of kernel derived CFP (filled circles) and the net CFP obtained from the Gregory regression technique (filled triangles). Strong agreement between both methods indicate that kernel ensemble mean is accurately capturing the extent of net TOA flux perturbation as outputted directly from the models.

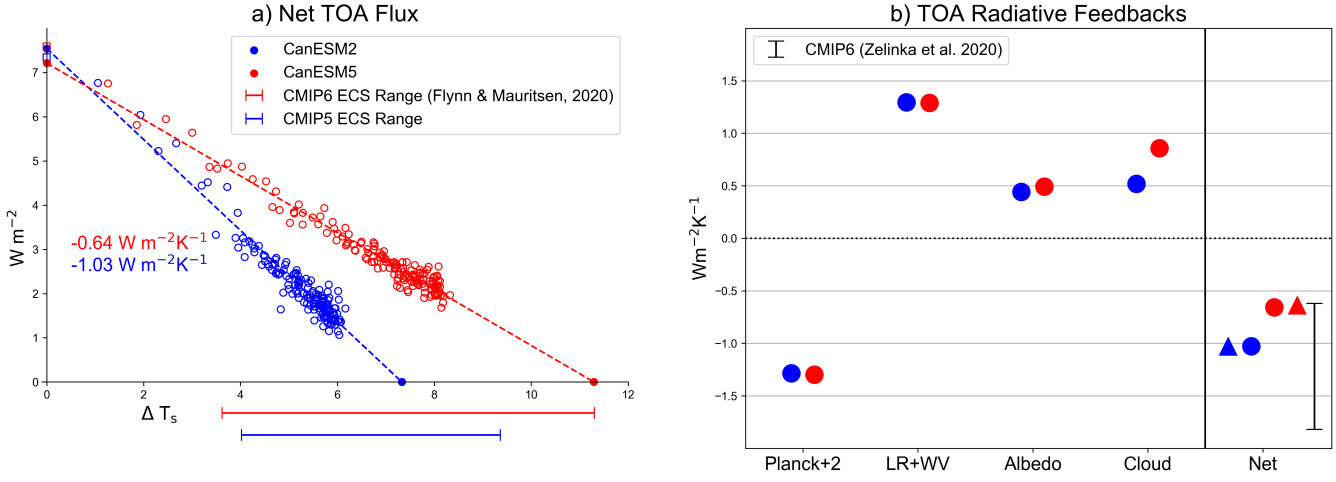

Figure 1. a) Net top-of-atmosphere (TOA) radiation plotted against global, annual mean surface air temperature change in abrupt-4xCO2 simulations for CanESM2 (blue) and CanESM5 (red). Standard 150 year Gregory regressions using net top-of-atmosphere radiative flux (adjusted by a preindustrial 150 year annual mean control climate) are conducted, where the x-axis intercept of the regression line divided by two is defined as the ECS, and the y-axis intercept is defined as the ERF. For comparison, the ERF, as calculated using fixed SST AMIP style runs, is shown for both versions of CanESM via the open squares along the y-axis. Bars below the x-axis denote the model range for ECS for both CMIP5 & CMIP6 (Flynn and Mauritsen, 2020). b) Global, annual mean top of atmosphere radiative feedbacks calculated using radiative kernels (in $Wm^{-2}K^{-1}$). From left to right, feedbacks are listed as Planck+2 (a value of 2 was added for display purposes to better illustrate differences in the other feedbacks), lapse rate plus water vapour, surface albedo, cloud, and net feedback. For comparison, we also show the net climate feedback value obtained using the standard Gregory regression approach (filled triangles), as well as the CMIP6 model range (Zelinka et al., 2020).

https://doi.org/10.5194/gmd-2021-11
Preprint. Discussion started: 8 March 2021

Geoscientific Model Development Discussions

The primary contribution to CanESM5's high ECS is a stronger cloud feedback (Figure 1b), in line with literature assessing causes behind the widespread increase in ECS from CMIP5 to CMIP6 (Flynn and Mauritsen, 2020; Zelinka et al., 2020; Gettelman et al., 2019; Andrews et al., 2019; Golaz et al., 2019). Given cloud feedbacks operate in both the shortwave (through their optical thickness and resultant albedo) and longwave (through their emissivity), we now decompose and examine its longwave and shortwave components separately below.

3.2.1 Cloud Feedbacks

The LW cloud feedback is positive for both versions of CanESM— increasing by 0.06 $Wm^{-2}K^{-1}$ from CanESM2 to 5 (Figure 3a). CanESM2 exhibits a negative SW cloud feedback (-0.21 $Wm^{-2}K^{-1}$), while in CanESM5 the SW cloud feedback has become weakly positive (0.06 $Wm^{-2}K^{-1}$), indicating an absolute difference of 0.27 $Wm^{-2}K^{-1}$ (Figure 3b). These results are insensitive to the selected kernel ensemble used with the adjusted-CRE method in our analysis, as the standard deviation across radiative kernels (as denoted by the error bars in Figure 3) is comparable for both versions of CanESM. Given that we have shown only modest differences in all other components of the forcing-feedback framework, cloud feedbacks, predominantly in the SW, emerge as the most likely source of increased ECS in CanESM5. Therefore, we devote the rest of this article to investigating the causes of this change by further decomposing both the SW and LW cloud feedbacks into their altitude, optical depth, and amount components. Although the change in net LW cloud feedback is small, we will demonstrate in the following section that, in fact, this is due to a subtle but important compensation between its individual components.

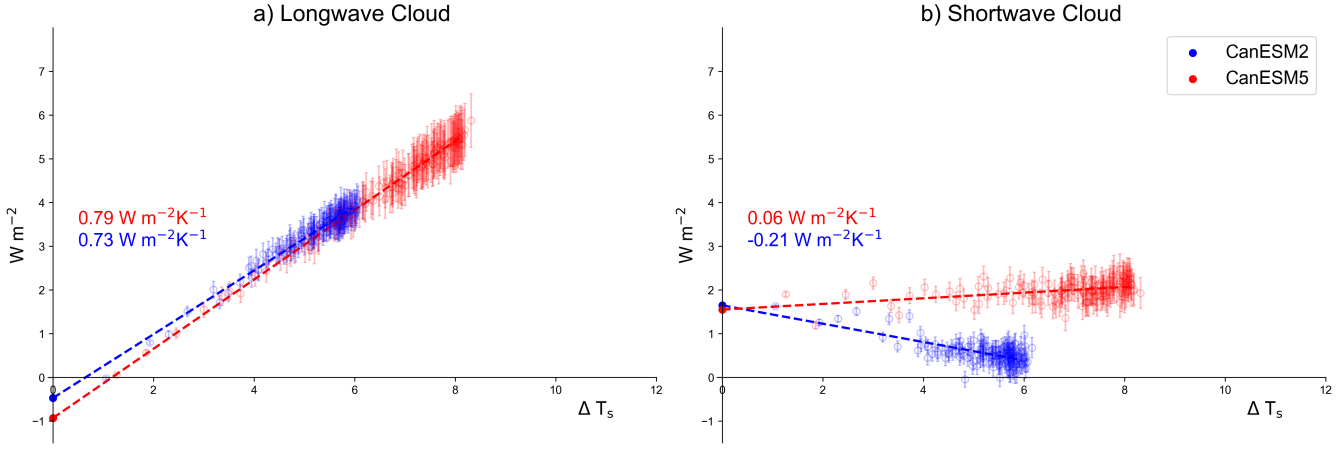

Figure 2. Cloud long- and shortwave flux plotted against global, annual mean surface temperature change in abrupt-4xCO2 simulations for CanESM2 (blue) and CanESM5 (red), calculated using the adjusted CRE method. Standard 150 year Gregory regressions are conducted, where the slope of the regression line equals the cloud feedback (in $Wm^{-2}K^{-1}$). Error bars denote ± one standard deviation across the selected radiative kernel ensemble.

https://doi.org/10.5194/gmd-2021-11
Preprint. Discussion started: 8 March 2021


Geoscientific Model Development Discussions

3.2.2 Decomposition

The SW cloud feedback arises due to changes in cloud amount and/or optical properties. Cloud optical thickness is dependent on water path and cloud droplet size distribution (Slingo, 1989). The phase composition of clouds (liquid, ice, or mixed) is linked strongly to their optical thickness due to liquid droplets and ice crystals having different characteristic size distributions, where clouds composed of predominantly smaller liquid droplets tend to be more reflective (Pruppacher and Klett, 1980). As a result, regions where cloud composition consists entirely of liquid droplets, or are mixed phase, tend to exhibit higher albedo. In terms of feedbacks, cloud phase and amount changes have been identified as an explanatory factor to ECS spread in ESMs (Tan et al., 2016; Zelinka et al., 2016). Thus, we now decompose the cloud feedbacks using cloud radiative kernels and ISCCP simulator output for each version of CanESM following the methods described in Zelinka et al. (2012a, b) to investigate individual cloud feedback processes. We apply the decomposition separately to low and non-low clouds.

In Figure 3, we decompose LW and SW cloud feedbacks into contributions from changes in cloud optical depth, cloud altitude, and cloud amount. The LW total cloud feedback is dominated by contributions from non-low clouds (Figure 3a), with small negative contributions from low clouds (Figure 3b). Changes in cloud optical depth or amount have little radiative influence for low clouds given low cloud top temperatures are close to that of the surface, resulting in similar outgoing longwave radiation (i.e. little greenhouse effect). Notably, the LW feedback for both CanESM2 and CanESM5 is anomalously high relative to the CFMIP2 ensemble (Zelinka et al., 2016) (Figure 3a). For CanESM2, contributions to the LW feedback are comparable for optical depth and amount feedbacks— with largest contribution coming from altitude. The altitude feedback arises from cloud emissivity properties, and therefore operates predominantly in the longwave for non-low clouds. Tropical free troposphere clouds rise and maintain cooler cloud top temperatures relative to the surface, thereby becoming more efficient at trapping outgoing longwave radiation (Zelinka and Hartmann, 2010; Gettelman and Sherwood, 2016). For CanESM5, the LW feedback is approximately equal to CanESM2, albeit with larger contributions from optical depth and altitude feedbacks, and a smaller contribution from amount feedback. For low clouds, the LW feedbacks are all small in magnitude. The residuals (yellow) are small in both models (Figure 3), indicating that nonlinear processes are less important for understanding the changes between models.

In the SW, both models exhibit strong negative feedbacks for non-low clouds and strong positive feedbacks for low clouds (Figure 3). The negative non-low cloud shortwave feedback is driven by an increase in cloud amount and optical depth with warming. This result is consistent with both modelling and theoretical understanding of non-low cloud responses to warming. Specifically, an increasing number of liquid droplets relative to ice crystals gives rise to more mixed phase clouds, as well as increases the proportion of liquid to ice in existing mixed phase clouds, resulting in an higher optical depth (Senior and Ingram, 1989), and a positive relationship between mid latitude cloud liquid water content and the slope of the moist adiabat as the troposphere warms (i.e. a function of temperature) (Betts, 1987). The situation for the non-low cloud SW feedback is similar to that of the LW feedback, in that it is anomalously strong for CanESM2 relative to the CFMIP2 ensemble (Zelinka et al., 2016) (Figure 3a). For low clouds, the SW is dominated by a strong positive amount feedback (decrease in cloudiness), with a small negative contribution from optical depth feedback (increase in cloud optical depth) (Figure 3b). For CanESM5,

https://doi.org/10.5194/gmd-2021-11
Preprint. Discussion started: 8 March 2021

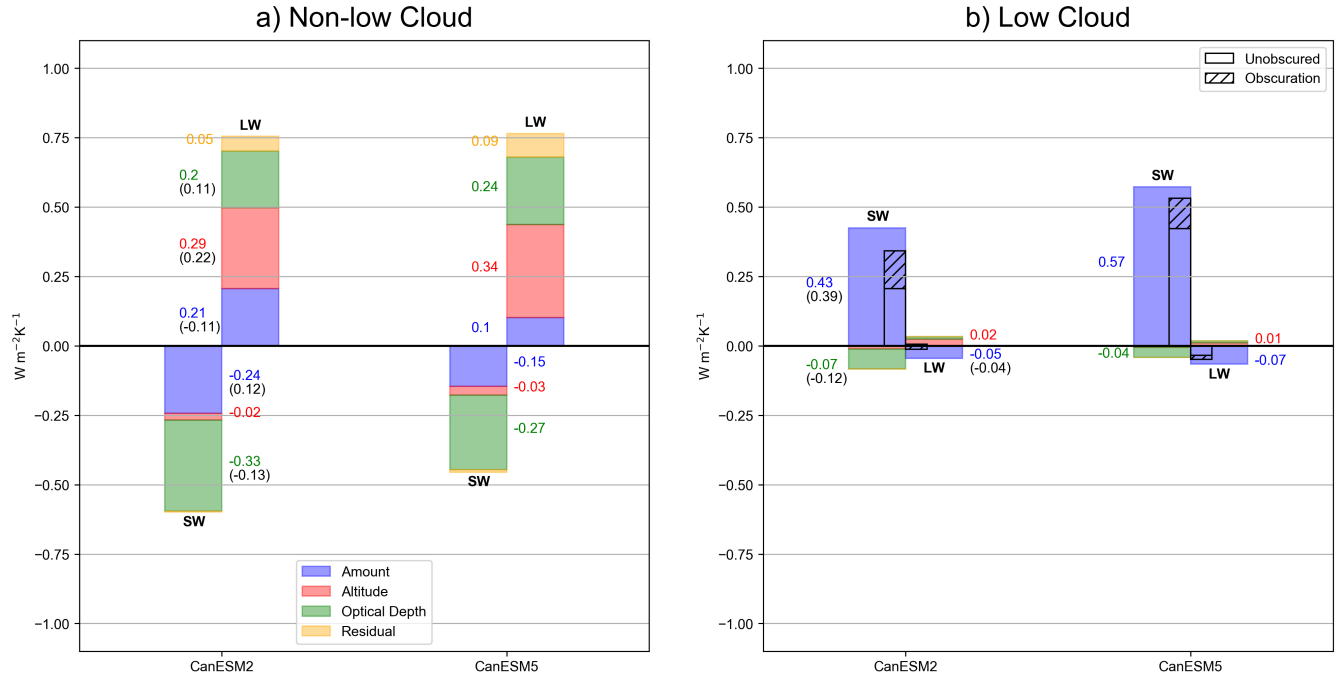

Figure 3. Global, annual mean decomposed cloud feedbacks for CanESM2 & CanESM5. Feedbacks are partitioned into both LW and SW contributions from cloud amount (blue), cloud altitude (red), optical depth (green), and residual (orange) terms, for non-low (panel a) and low clouds (panel b). Low cloud feedbacks are also separated via non-obscured and obscuration terms in black bars in panel b. For contributions smaller than 0.01 $Wm^{-2}K^{-1}$, text values were omitted for the sake of clarity. Black values in parentheses indicate multi-model mean values from the CFMIP1/CFMIP2 ensemble (Zelinka et al., 2016).

SW feedbacks differ from CanESM2 considerably for both non-low and low clouds. For non-low clouds, CanESM5's optical depth feedback is weaker (less negative) than CanESM2 (+0.06 $Wm^{-2}K^{-1}$) (Figure 3a). While the SW non-low cloud amount feedback is also weaker in CanESM5, the difference is offset in the LW. For low clouds, the SW amount feedback exhibits the largest difference between the two model versions (+0.14 $Wm^{-2}K^{-1}$). The change in SW cloud feedback strength and sign between CanESM2 and CanESM5 is related to multiple feedback mechanisms operating at different cloud heights. The largest contributor is the SW low cloud amount feedback, which is more positive in CanESM5. Changes in optical depth feedbacks are mainly important for non-low clouds, and are less negative in CanESM5.

The large difference in SW low cloud feedback strength between CanESM2 and CanESM5 raises the possibility that a portion of what the COSP interprets as a low cloud response is actually the result of changes in the spatial distribution of non-low cloud fraction under climate change; a phenomenon known as 'obscuration' (Zelinka et al., 2018). The black bars in Figure 3b indicate the both CanESM2 and CanESM5 have a non-negligible obscuration term. However, given that the extent of obscuration is similar between both versions of CanESM (see hatched bars in Figure 3b), it does not appear to be a major contributor to increased feedback strength in CanESM5 relative to CanESM2.

https://doi.org/10.5194/gmd-2021-11
Preprint. Discussion started: 8 March 2021

3.2.3 Spatial Distribution

Low cloud amount feedbacks are considered a robust positive feedback mechanism diagnosed from both observational and modelling studies, albeit with substantial inter-model spread in terms of strength (Eitzen et al., 2011; Clement et al., 2009; Zelinka et al., 2016). The low cloud amount feedback is closely tied to the distribution of marine stratiform cloud regimes persisting in the sub/tropics over ocean eastern boundary current regions (Klein et al., 2017). The non-low cloud optical depth feedback has been shown to have rich- and sometimes offsetting- spatial structure, owing to mostly negative feedback mid/high latitudes and a rich zonal structure at low latitudes (Zelinka et al., 2012b, 2016). As such, we now examine the spatial distribution of both the SW low cloud amount and non-low cloud optical depth feedbacks (Figure 4).

Figure 4 shows annual mean SW non-low cloud optical depth and low cloud amount feedbacks for CanESM2 and CanESM5. The SW non-low cloud optical depth feedback is negative in CanESM2 & 5 (Figure 4a and c), with minima over the western tropical Pacific Ocean. For the SW low cloud amount feedback, both models are strongest over subtropical/tropical Eastern Ocean basins and across the equatorial Pacific (Figure 4b and d). Notably, these regions have persistent low, stratiform cloud regimes, which are closely tied to strong temperature inversions that cap the PBL (Klein and Hartmann, 1993).

For CanESM5, increases in SW non-low cloud optical depth feedback are exhibited throughout the subtropical Pacific and tropical Eastern Pacific Ocean (Figure 4e). While there is strong positive (negative) feedback over the Eastern Indian (Western Pacific) Ocean, it is offset by a similar strength and opposing sign in the LW (not shown), and so it does not influence the global mean net (LW+SW). For SW low cloud amount feedback, CanESM5 exhibits an increase over CanESM2 in every region of persistent low cloud cover regimes, as well as across the eastern equatorial pacific and the western ocean basin off the Brazilian coast, relating to the simulation of substantially reduced LCC under a warming climate (Figure 4f).

Multiple lines of evidence from modelling studies have linked the sensitivity of LCC over the oceans to local changes in SST (Zhou et al., 2017; Andrews and Webb, 2018). Furthermore, the evolving spatial pattern of surface warming from interannual to centennial time scales is associated with differences between interannual and long term cloud feedback strength (Zhou et al., 2015). The underlying physical mechanisms linking local surface warming to reduced LCC are: 1) increased surface latent heat flux dries and deepens the boundary layer via increased buoyancy-driven turbulence and resultant downward mixing from free troposphere air (Qu et al., 2015; Rieck et al., 2012), and 2) increased surface specific humidity promotes further moisture contrast between the boundary layer and the free troposphere such that when air is mixed downward it is relatively drier (Van der Dussen et al., 2015; Qu et al., 2015). As such, we now turn to an analysis of the cloud feedbacks in both CanESM2 and CanESM5 under prescribed sea surface boundary conditions in order to investigate the influence local SST changes to CanESM5's SW cloud feedbacks and how they differ from CanESM2.

3.3 Influence of the Spatial Pattern of SST Changes

To investigate the spatial pattern of warming and its influence on SW cloud feedbacks, we use two additional experiments from the CFMIP Tier 1 experiment deck— amip-p4K and amip-future4K (Webb et al., 2017). In amip-p4K, a globally uniform SST perturbation of +4 K is applied relative to the standard amip DECK experiment from CMIP6. In amip-future4K, a patterned

https://doi.org/10.5194/gmd-2021-11
Preprint. Discussion started: 8 March 2021

Geoscientific Model Development Discussions

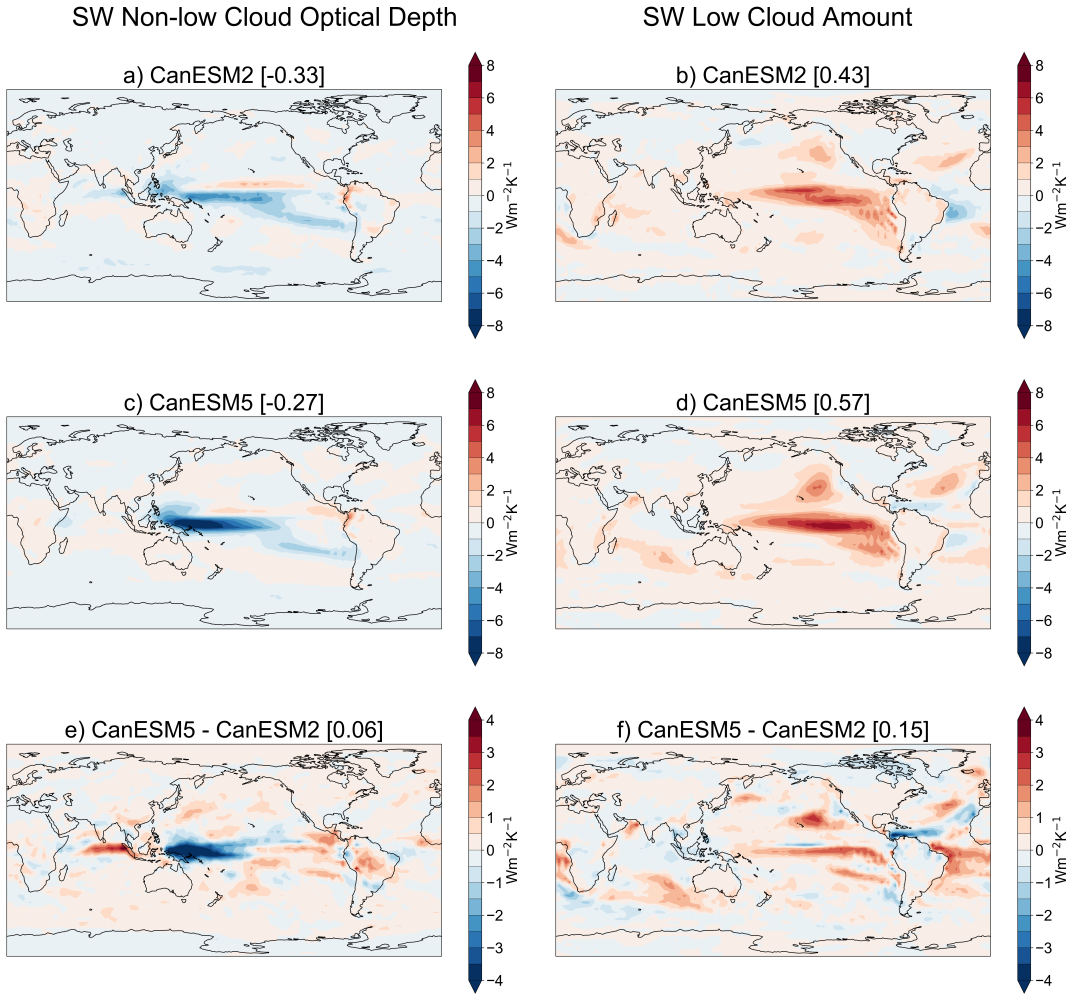

Figure 4. Annual mean SW non-low cloud optical depth (left) and SW low cloud amount (right) feedbacks for CanESM2 (panels a & b) and CanESM5 (panels c & d). Panels e & f show the difference between CanESM5 & CanESM2 for each respective feedback. Values in square brackets next to each subplot title denote the global mean value for each respective map. Note the difference in colour bar scales for top and bottom/middle panels.

warming perturbation, derived from multi-model mean coupled ESM warming patterns, is applied to the standard amip DECK experiment and then scaled such that the global mean SST perturbation is +4 K. Sea ice concentration is held fixed to the control amip deck experiment. Analysis of cloud feedbacks in these two experiments allows for comparison between CanESM2 and 5 under identical SST forcing (Figure A4), which helps to isolate the contribution to change in cloud feedbacks that arises due to changes in the atmosphere model (CanAM4 to CanESM5) independent of the ocean model replacement (NCAR CSM to CanNEMO).

https://doi.org/10.5194/gmd-2021-11
Preprint. Discussion started: 8 March 2021

Geoscientific Model Development Discussions

In both amip experiments, CanESM2 exhibits strong non-low cloud feedbacks in both the SW and LW (Figure 5). The result is a near cancellation and slightly positive non-low cloud feedback for both amip-p4K (0.11 $Wm^{-2}K^{-1}$) and amip-future4k (0.14 $Wm^{-2}K^{-1}$). Similarly, while individual LW and SW feedbacks differ, the net non-low cloud feedback in CanESM5 is comparable across both amip experiments (0.26 and 0.25 $Wm^{-2}K^{-1}$ for amip-p4K and amip-future4K, respectively) (Figure 5a and c). Relative to CanESM2, CanESM5 exhibits an overall less negative non-low cloud feedback of comparable magnitude to feedbacks derived from abrupt-4xCO_2 runs, mostly due to changes in SW amount and optical depth.

For low clouds, both versions of CanESM have a more positive SW feedback in amip-future4K experiment relative to amip-p4K (Figure 5b & d); this result is consistent with theoretical understanding relating warmer local SSTs to reduced boundary layer marine cloud cover as outlined in the previous section. Of cloud feedbacks partitioned into LW/SW and non-low/ unobscured low, the SW low cloud feedback is well correlated with tropical SST pattern anomalies in the amip-future4K experiment (Figure 6). However, amip-p4K's spatially uniform surface warming, its strong low cloud feedback suggests it can be primarily explained by underlying SST climatology, which has a direct influence on the extent of lower tropospheric convective mixing, and therefore LCC (Sherwood et al., 2014). Prior to accounting for the obscuring effects of overlying free troposphere clouds, the SW low cloud feedback is similar for both CanESM2 and CanESM5 (Figure 5). However, once obscuring effects are separated, CanESM5 exhibits a more positive SW low cloud feedback— similar to feedbacks from simulations with interactive ocean models (Figure 5b & d).

In contrast to feedbacks from abrupt-4xCO_2 runs, the extent of obscuration from free troposphere clouds differs between CanESM2 and 5 (Figure 5b & d). Under the assumption that the obscuration term can be considered a part of the non-low cloud feedback, feedbacks derived from the amip experiments exhibit some differences those with interactive SSTs (abrupt-4xCO_2) in both versions of CanESM for non-low and low clouds. However, for all experiments, the net cloud feedback remains more positive in CanESM5, ranging from +0.17 $Wm^{-2}K^{-1}$ (amip-future4k) to +0.29 $Wm^{-2}K^{-1}$ (abrupt-4xCO_2) (Table 1).

4 Discussion & Conclusions

Table 1. Summary of cloud feedback results, calculated using cloud radiative kernels, from abrupt-4xCO_2, amip-p4K, and amip-future-4K experiments for both CanESM2 and CanESM5 in this study. For this summary table, obscuring effects on low clouds have been counted as a non-low cloud feedback. Individual cell format: non-low / unobscured low / **net** (in $Wm^{-2}K^{-1}$)

	Experiment		
Model	abrupt-4xCO_2	amip-future4K	amip-p4K
CanESM2	0.28 / 0.22 / **0.50**	0.29 / 0.33 / **0.62**	0.23 / 0.27 / **0.50**
CanESM5	0.40 / 0.39 / **0.79**	0.36 / 0.43 / **0.79**	0.32 / 0.39 / **0.71**

In this study, we have analyzed both forcing and feedback in idealized experiments with instantaneous quadrupling of atmospheric CO_2 (abrupt-4xCO_2) using two versions of CanESM to elucidate the underlying cause behind CanESM5's increased

https://doi.org/10.5194/gmd-2021-11
Preprint. Discussion started: 8 March 2021

Geoscientific Model Development Discussions
Open Access
EGU

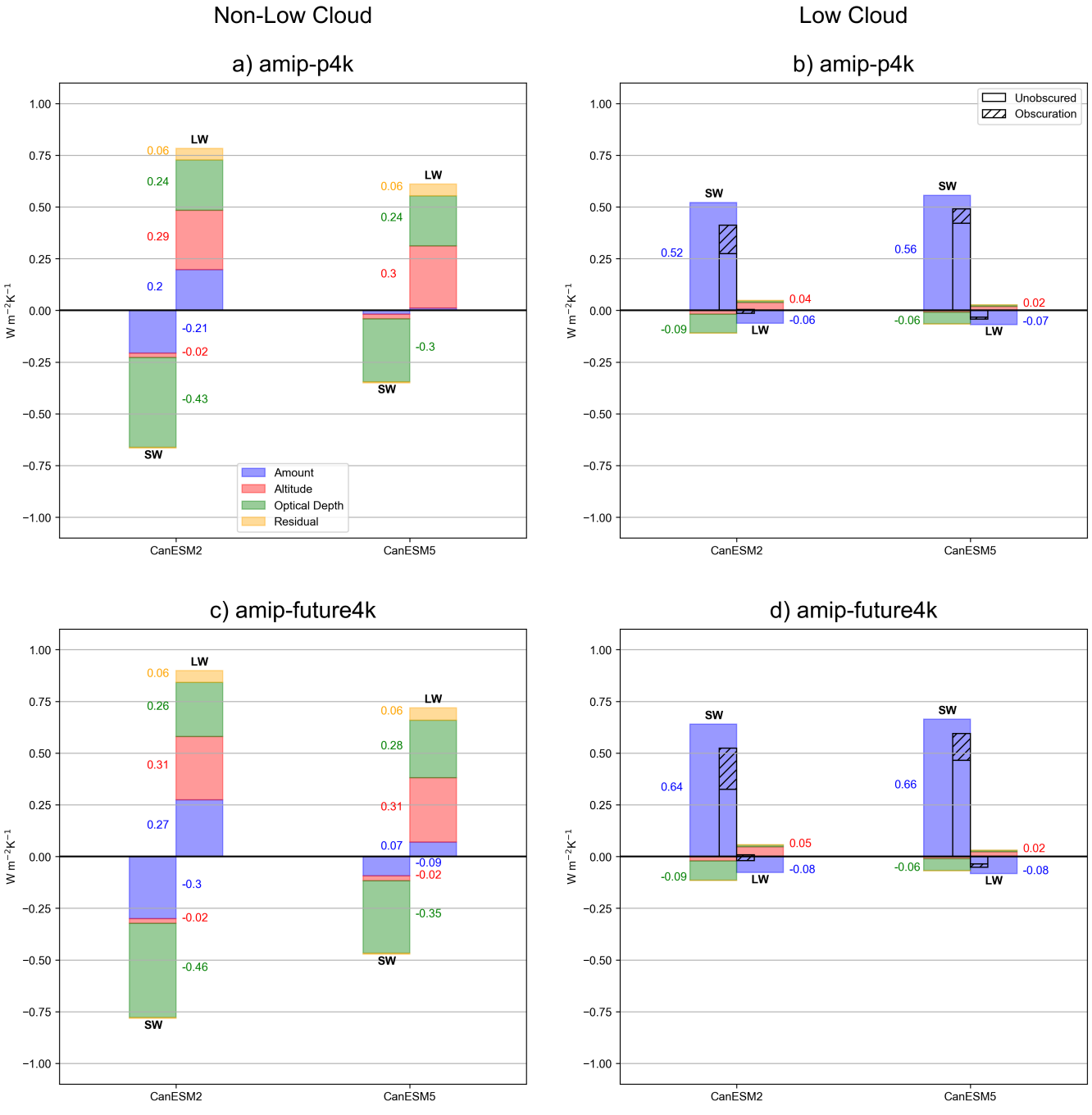

Figure 5. As in Figure 3, but for amip-p4K and amip-future4K experiments.

ECS (5.65 K). Using radiative kernels and output from RFMIP, we find only modest differences in both forcing and non-cloud

https://doi.org/10.5194/gmd-2021-11
Preprint. Discussion started: 8 March 2021

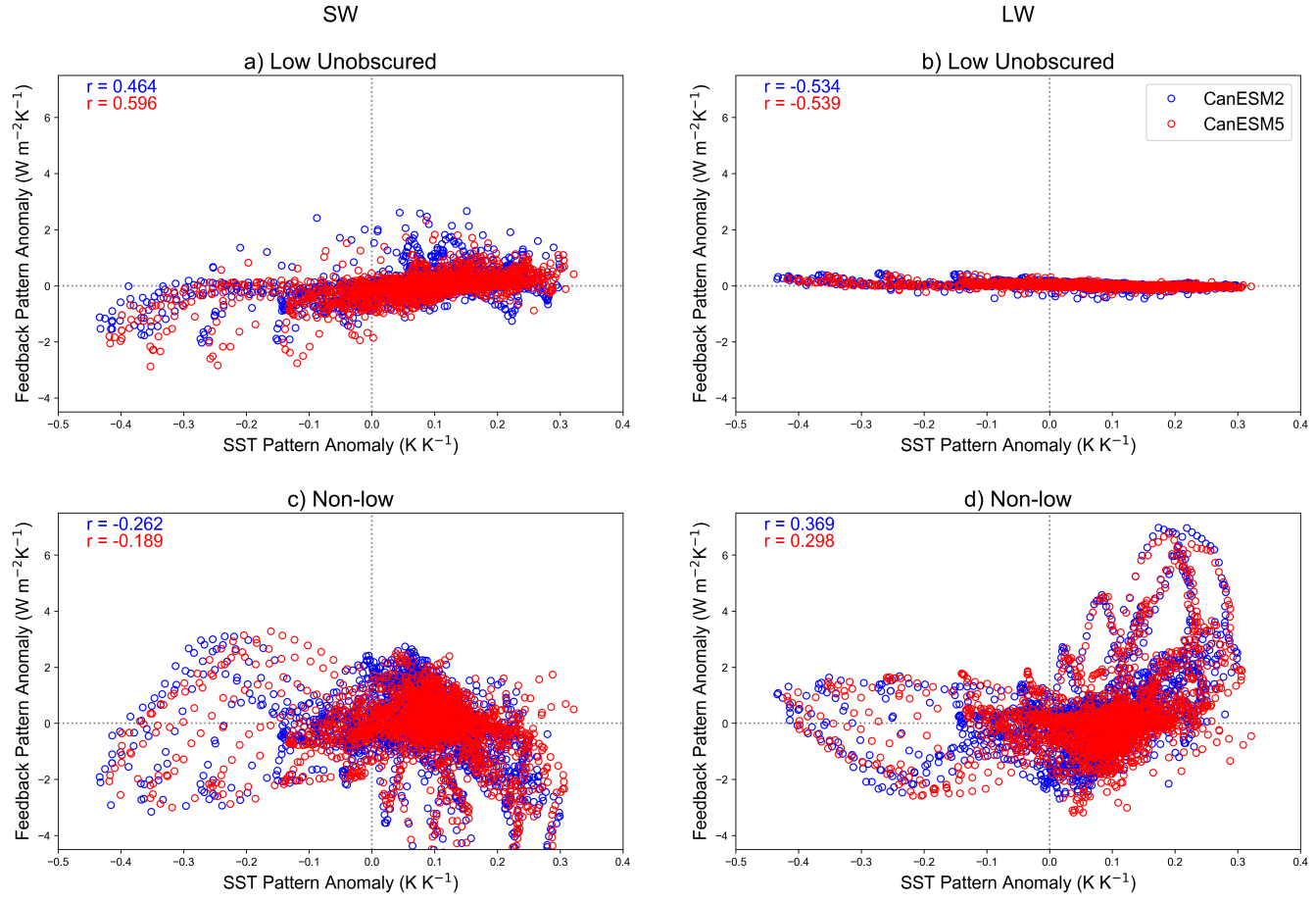

Figure 6. Relationship between tropical SW low non obscured cloud feedback and TS pattern anomalies. Pattern anomalies are measured as the difference between amip-future4K and amip-p4K SST perturbation experiments, where local TS responses are normalized by the global mean SST change (4 K). Here, data points are taken from 30N to 30S over the ocean.

feedbacks. The largest difference in feedback strength between CanESM2 to CanESM5 is from the cloud feedback, particularly in the SW. Further breakdown of the cloud feedback into its individual components (optical depth, altitude, and amount) at distinct cloud top heights (<680 hPa for non-low, ≥680 hPa for low) revealed that the SW low cloud amount and non-low cloud optical depth feedbacks are the dominant contributor to CanESM5's increased ECS (+0.14 and 0.06 $Wm^{-2}K^{-1}$, respectively) in abrupt 4x-CO_2 simulations. Analysis of the spatial pattern for each feedback showed the largest model differences in SW low cloud amount feedback over subtropical eastern ocean basins and across the equatorial pacific ocean, and in SW non-low optical depth feedback over the subtropical and extratropical pacific ocean.

We analyzed the spatial pattern of surface warming in CanESM5 and its influence on the SW low cloud feedback using two amip experiments with prescribed SSTs and sea ice (amip-p4K and amip-future4K). The tropical pattern anomaly of warming

https://doi.org/10.5194/gmd-2021-11
Preprint. Discussion started: 8 March 2021


Geoscientific Model Development Discussions

from the coupled model (relative to spatially uniform warming) is well correlated with the SW low cloud feedback— in agreement with studies linking warmer (colder) SSTs to decreased (increased) LCC (Qu et al., 2014; Bretherton and Blossey, 2014; Brient and Schneider, 2016), as well as the more positive feedback in patterned surface warming experiments. Furthermore, we found non negligible differences in the magnitude of amip derived cloud feedbacks from those in abrupt-4xCO_2 simulations, particularly for non-low clouds. However, when summed to yield a net cloud feedback, CanESM5 exhibits a more positive cloud feedback regardless of the experiment design analyzed in this study (Table 1); this result is noteworthy from a model development perspective given that CanESM2 and CanESM5 have distinct ocean models (CanNEMO for CanESM5 (Swart et al., 2019) and the National Centre for Atmospheric Research CSM ocean model for CanESM2 (Gent et al., 1998)).

Our results add further evidence the recent trend of several ESMs participating in CMIP6 exhibiting higher ECS than their CMIP5 counterpart— predominantly due to changes in SW cloud feedback strength and/or aerosol-cloud interactions (Gettelman et al., 2019; Andrews et al., 2019; Bodas-Salcedo et al., 2019). However, it is worth noting that several modelling centres report increased ECS sourced from distinct developments in newer versions of their respective model (e.g. addition of a mixed-phase cloud scheme and improved aerosol-cloud interactions in HadGEM3-GC2.0 (Bodas-Salcedo et al., 2019; Mulcahy et al., 2018). Attribution of CanESM5's increase in ECS to specific model developments is a subject for future work, including cloud microphysics, aerosols, and their interactions. However, our analysis using simulations with prescribed SSTs still showed a stronger cloud feedback, suggesting that the ocean model is not the primary factor explaining this increase.

Finally, we emphasize that the results presented in this study do not seek to comment on the plausibility of climate sensitivity from either version of CanESM. Recently, there has been an expansion of work relating constraints on climate sensitivity through the use of the satellite and paleoclimate observational records (Sherwood et al., 2020). Furthermore, there are limitations of interpreting the validity of climate sensitivity results (as calculated here) due to uncertainties associated with statistical methods (e.g. assuming a time-invariant climate sensitivity parameter via the regression approach) (Gregory et al., 2004). However, we reiterate the scope of this study: establishing a causal link for the increased climate sensitivity from CanESM2 to CanESM5 under long term, idealized climate change.

Code and data availability. All model output from both versions of the Canadian Earth System Model analyzed in this study are publicly available for download via the Earth System Grid Federation (https://esgf-node.llnl.gov/projects/esgf-llnl/). Source code for the Canadian Earth System model can be found at https://gitlab.com/cccma/canesm. The particular model version (5.0.3) that contributed output to CMIP6 is available from https://doi.org/10.5281/zenodo.3251113. Code used for analysis of model output and production of figures is located at https://github.com/JohnVirgin/GMD_CanESM_Clouds.

https://doi.org/10.5194/gmd-2021-11
Preprint. Discussion started: 8 March 2021

Geoscientific Model Development Discussions
Open Access
EGU

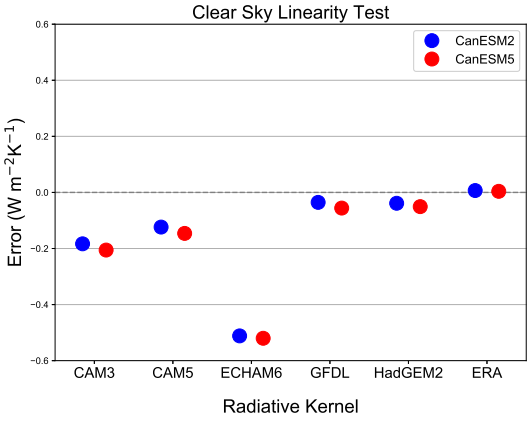

Figure A1. Clear sky linearity test for 6 sets of radiative kernels considered in this study (CAM3, CAM5, ECHAM6, HadGEM2, and ERA kernels) tested using each version of CanESM. Y-axis error is defined as the absolute difference between the Gregory regression derived net clear sky climate feedback parameter, and radiative kernel derived net clear sky climate feedback parameter.

https://doi.org/10.5194/gmd-2021-11
Preprint. Discussion started: 8 March 2021

Geoscientific Model Development Discussions
Open Access
EGU

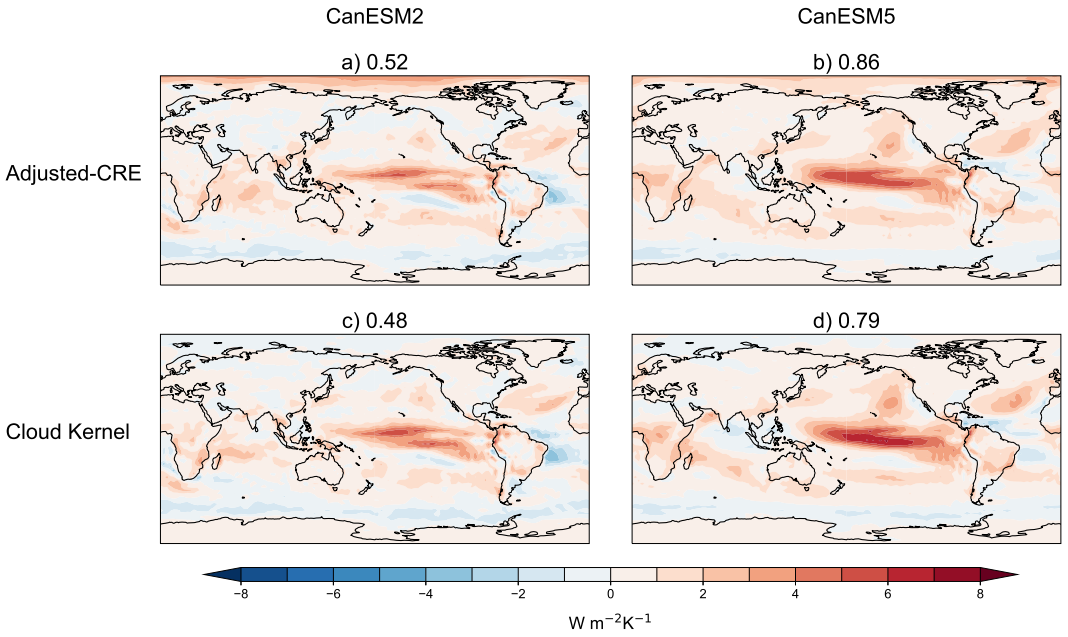

Figure A2. Comparison of annual mean net cloud feedbacks for CanESM2 (panels a & c) and CanESM5 (panels b &d), calculated using the adjusted-CRE method and the cloud kernel method. Global mean values are shown in square brackets next to each subplot title. CanESM2 Pearson's $r = 0.72$ ($p < 0.01$); CanESM5 Pearson's $r = 0.86$ ($p < 0.01$).

https://doi.org/10.5194/gmd-2021-11
Preprint. Discussion started: 8 March 2021

Geoscientific Model Development Discussions
Open Access
EGU

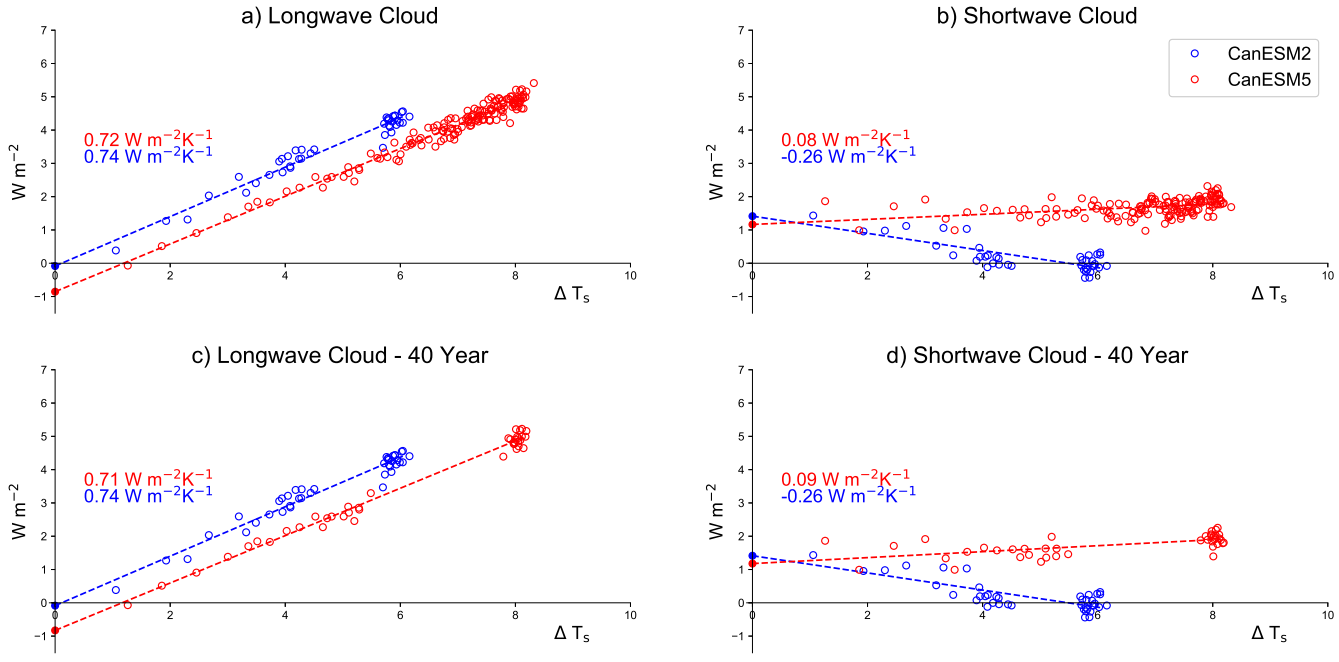

Figure A3. As in Figure 2, but feedbacks are calculated using the standard cloud kernel method as opposed to the adjusted-CRE method. Panels a & b show regressions using all available years of data for each model version, whereas panels c & d show subsampled data for CanESM5 (years 1-20 & 120-140).

https://doi.org/10.5194/gmd-2021-11
Preprint. Discussion started: 8 March 2021

Geoscientific Model Development Discussions
Open Access
EGU

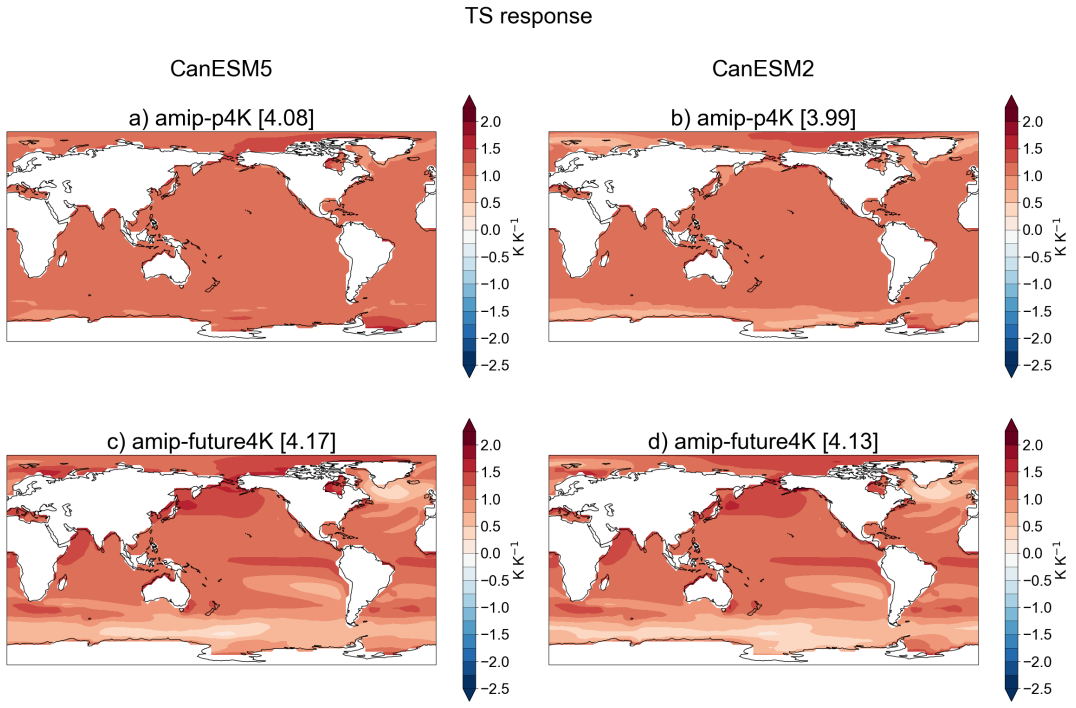

Figure A4. Global, annual mean amip-p4K and amip-future4K surface temperature response for both CanESM2 and CanESM5. Global mean values are shown in square brackets next to each subplot title, where values over land surfaces were excluded in cosine area weighted averaging. For both experiments, differences were calculated using a temporal mean spanning the simulation's entire length (36 years) and then divided by the corresponding global mean value.

https://doi.org/10.5194/gmd-2021-11
Preprint. Discussion started: 8 March 2021


Geoscientific Model Development Discussions

Author contributions. JGV performed analysis on model output and created all figures used in this study. JGV, CGF, JC, KVS, and TM wrote the manuscript.

Competing interests. The authors declare that there are no competing interests.

Acknowledgements. The authors acknowledge Mark Zelinka, Neil Swart, and Nathan Gillet for providing useful insights and comments that helped improve this study. The authors also acknowledge the World Climate Research Programme's (WCRP) Working Group on Coupled Modelling (WGCM) and the Earth system Grid Federation (ESGF) for their role in providing access to the data used in this study.

https://doi.org/10.5194/gmd-2021-11
Preprint. Discussion started: 8 March 2021

References

Andrews, T. and Webb, M. J.: The dependence of global cloud and lapse rate feedbacks on the spatial structure of tropical Pacific warming, Journal of Climate, 31, 641–654, 2018.

Andrews, T., Gregory, J. M., Webb, M. J., and Taylor, K. E.: Forcing, feedbacks and climate sensitivity in CMIP5 coupled atmosphere-ocean climate models, Geophysical Research Letters, 39, 2012.

Andrews, T., Andrews, M. B., Bodas-Salcedo, A., Jones, G. S., Kuhlbrodt, T., Manners, J., Menary, M. B., Ridley, J., Ringer, M. A., Sellar, A. A., et al.: Forcings, feedbacks, and climate sensitivity in HadGEM3-GC3. 1 and UKESM1, Journal of Advances in Modeling Earth Systems, 11, 4377–4394, 2019.

Arora, V., Boer, G., Christian, J., Curry, C., Denman, K., Zahariev, K., Flato, G., Scinocca, J., Merryfield, W., and Lee, W.: The effect of terrestrial photosynthesis down regulation on the twentieth-century carbon budget simulated with the CCCma Earth System Model, Journal of Climate, 22, 6066–6088, 2009.

Arora, V., Scinocca, J., Boer, G., Christian, J., Denman, K., Flato, G., Kharin, V., Lee, W., and Merryfield, W.: Carbon emission limits required to satisfy future representative concentration pathways of greenhouse gases, Geophysical Research Letters, 38, 2011.

Betts, A. K.: Thermodynamic constraint on the cloud liquid water feedback in climate models, Journal of Geophysical Research: Atmospheres, 92, 8483–8485, 1987.

Bjordal, J., Storelvmo, T., Alterskjær, K., and Carlsen, T.: Equilibrium climate sensitivity above 5 ° C plausible due to state-dependent cloud feedback, Nature Geoscience, pp. 1–4, 2020.

Block, K. and Mauritsen, T.: Forcing and feedback in the MPI-ESM-LR coupled model under abruptly quadrupled CO2, Journal of Advances in Modeling Earth Systems, 5, 676–691, 2013.

Blossey, P. N., Bretherton, C. S., Zhang, M., Cheng, A., Endo, S., Heus, T., Liu, Y., Lock, A. P., de Roode, S. R., and Xu, K.-M.: Marine low cloud sensitivity to an idealized climate change: The CGILS LES intercomparison, Journal of Advances in Modeling Earth Systems, 5, 234–258, 2013.

Bodas-Salcedo, A., Webb, M., Bony, S., Chepfer, H., Dufresne, J.-L., Klein, S., Zhang, Y., Marchand, R., Haynes, J., Pincus, R., et al.: COSP: Satellite simulation software for model assessment, Bulletin of the American Meteorological Society, 92, 1023–1043, 2011.

Bodas-Salcedo, A., Mulcahy, J., Andrews, T., Williams, K., Ringer, M., Field, P., and Elsaesser, G.: Strong dependence of atmospheric feedbacks on mixed-phase microphysics and aerosol-cloud interactions in HadGEM3, Journal of Advances in Modeling Earth Systems, 11, 1735–1758, 2019.

Bretherton, C. S. and Blossey, P. N.: Low cloud reduction in a greenhouse-warmed climate: Results from Lagrangian LES of a subtropical marine cloudiness transition, Journal of Advances in Modeling Earth Systems, 6, 91–114, 2014.

Bretherton, C. S., Blossey, P. N., and Jones, C. R.: Mechanisms of marine low cloud sensitivity to idealized climate perturbations: A single-LES exploration extending the CGILS cases, Journal of Advances in Modeling Earth Systems, 5, 316–337, 2013.

Brient, F. and Schneider, T.: Constraints on climate sensitivity from space-based measurements of low-cloud reflection, Journal of Climate, 29, 5821–5835, 2016.

Caldwell, P. M., Zelinka, M. D., Taylor, K. E., and Marvel, K.: Quantifying the sources of intermodel spread in equilibrium climate sensitivity, Journal of Climate, 29, 513–524, 2016.

Ceppi, P., Brient, F., Zelinka, M. D., and Hartmann, D. L.: Cloud feedback mechanisms and their representation in global climate models, Wiley Interdisciplinary Reviews: Climate Change, 8, e465, 2017.

https://doi.org/10.5194/gmd-2021-11
Preprint. Discussion started: 8 March 2021

Charney, J. G., Arakawa, A., Baker, D. J., Bolin, B., Dickinson, R. E., Goody, R. M., Leith, C. E., Stommel, H. M., and Wunsch, C. I.: Carbon Dioxide and Climate: A Scientific Assessment, National Academies Press, Washington, DC, https://doi.org/10.17226/12181, https://doi.org/10.17226%2F12181, 1979.

Chung, E.-S. and Soden, B. J.: An assessment of direct radiative forcing, radiative adjustments, and radiative feedbacks in coupled ocean–atmosphere models, Journal of Climate, 28, 4152–4170, 2015.

Clement, A. C., Burgman, R., and Norris, J. R.: Observational and model evidence for positive low-level cloud feedback, Science, 325, 460–464, 2009.

Dufresne, J.-L. and Bony, S.: An assessment of the primary sources of spread of global warming estimates from coupled atmosphere–ocean models, Journal of Climate, 21, 5135–5144, 2008.

Eitzen, Z. A., Xu, K.-M., and Wong, T.: An estimate of low-cloud feedbacks from variations of cloud radiative and physical properties with sea surface temperature on interannual time scales, Journal of climate, 24, 1106–1121, 2011.

Eyring, V., Bony, S., Meehl, G. A., Senior, C. A., Stevens, B., Stouffer, R. J., and Taylor, K. E.: Overview of the Coupled Model Intercomparison Project Phase 6 (CMIP6) experimental design and organization, Geoscientific Model Development, 9, 1937–1958, 2016.

Flynn, C. M. and Mauritsen, T.: On the climate sensitivity and historical warming evolution in recent coupled model ensembles, Atmospheric Chemistry & Physics, 20, 7829–7842, 2020.

Forster, P. M., Andrews, T., Good, P., Gregory, J. M., Jackson, L. S., and Zelinka, M.: Evaluating adjusted forcing and model spread for historical and future scenarios in the CMIP5 generation of climate models, Journal of Geophysical Research: Atmospheres, 118, 1139–1150, 2013.

Gent, P. R., Bryan, F. O., Danabasoglu, G., Doney, S. C., Holland, W. R., Large, W. G., and McWilliams, J. C.: The NCAR climate system model global ocean component, Journal of Climate, 11, 1287–1306, 1998.

Gettelman, A. and Sherwood, S.: Processes responsible for cloud feedback, Current Climate Change Reports, 2, 179–189, 2016.

Gettelman, A., Hannay, C., Bacmeister, J., Neale, R., Pendergrass, A., Danabasoglu, G., Lamarque, J.-F., Fasullo, J., Bailey, D., Lawrence, D., et al.: High climate sensitivity in the Community Earth System Model version 2 (CESM2), Geophysical Research Letters, 46, 8329–8337, 2019.

Golaz, J.-C., Caldwell, P. M., Van Roekel, L. P., Petersen, M. R., Tang, Q., Wolfe, J. D., Abeshu, G., Anantharaj, V., Asay-Davis, X. S., Bader, D. C., et al.: The DOE E3SM coupled model version 1: Overview and evaluation at standard resolution, Journal of Advances in Modeling Earth Systems, 11, 2089–2129, 2019.

Goosse, H., Kay, J. E., Armour, K. C., Bodas-Salcedo, A., Chepfer, H., Docquier, D., Jonko, A., Kushner, P. J., Lecomte, O., Massonnet, F., et al.: Quantifying climate feedbacks in polar regions, Nature communications, 9, 1–13, 2018.

Gregory, J., Ingram, W., Palmer, M., Jones, G., Stott, P., Thorpe, R., Lowe, J., Johns, T., and Williams, K.: A new method for diagnosing radiative forcing and climate sensitivity, Geophysical research letters, 31, 2004.

Hansen, J., Sato, M., Ruedy, R., Nazarenko, L., Lacis, A., Schmidt, G., Russell, G., Aleinov, I., Bauer, M., Bauer, S., et al.: Efficacy of climate forcings, Journal of Geophysical Research: Atmospheres, 110, 2005.

Huang, Y., Xia, Y., and Tan, X.: On the pattern of CO2 radiative forcing and poleward energy transport, Journal of Geophysical Research: Atmospheres, 122, 10–578, 2017.

Klein, S. A. and Hartmann, D. L.: The seasonal cycle of low stratiform clouds, Journal of Climate, 6, 1587–1606, 1993.

Klein, S. A., Hall, A., Norris, J. R., and Pincus, R.: Low-cloud feedbacks from cloud-controlling factors: a review, in: Shallow Clouds, Water Vapor, Circulation, and Climate Sensitivity, pp. 135–157, Springer, 2017.

https://doi.org/10.5194/gmd-2021-11
Preprint. Discussion started: 8 March 2021

Knutti, R., Rugenstein, M. A., and Hegerl, G. C.: Beyond equilibrium climate sensitivity, Nature Geoscience, 10, 727–736, 2017.

Mulcahy, J., Jones, C., Sellar, A., Johnson, B., Boutle, I., Jones, A., Andrews, T., Rumbold, S., Mollard, J., Bellouin, N., et al.: Improved aerosol processes and effective radiative forcing in HadGEM3 and UKESM1, Journal of Advances in Modeling Earth Systems, 10, 2786–2805, 2018.

Pendergrass, A. G., Conley, A., and Vitt, F. M.: Surface and top-of-atmosphere radiative feedback kernels for CESM-CAM5, Earth System Science Data, 10, 317–324, 2018.

Pincus, R., Forster, P. M., and Stevens, B.: The Radiative Forcing Model Intercomparison Project (RFMIP): experimental protocol for CMIP6, Geoscientific Model Development, 9, 3447–3460, https://doi.org/10.5194/gmd-9-3447-2016, https://gmd.copernicus.org/articles/9/3447/2016/, 2016.

Pruppacher, H. R. and Klett, J. D.: Microphysics of clouds and precipitation, Nature, 284, 88–88, 1980.

Qu, X., Hall, A., Klein, S. A., and Caldwell, P. M.: On the spread of changes in marine low cloud cover in climate model simulations of the 21st century, Climate dynamics, 42, 2603–2626, 2014.

Qu, X., Hall, A., Klein, S. A., and DeAngelis, A. M.: Positive tropical marine low-cloud cover feedback inferred from cloud-controlling factors, Geophysical Research Letters, 42, 7767–7775, 2015.

Rieck, M., Nuijens, L., and Stevens, B.: Marine boundary layer cloud feedbacks in a constant relative humidity atmosphere, Journal of the Atmospheric Sciences, 69, 2538–2550, 2012.

Rose, B. E., Armour, K. C., Battisti, D. S., Feldl, N., and Koll, D. D.: The dependence of transient climate sensitivity and radiative feedbacks on the spatial pattern of ocean heat uptake, Geophysical Research Letters, 41, 1071–1078, 2014.

Scott, R. C., Myers, T. A., Norris, J. R., Zelinka, M. D., Klein, S. A., Sun, M., and Doelling, D. R.: Observed Sensitivity of Low-Cloud Radiative Effects to Meteorological Perturbations over the Global Oceans, Journal of Climate, 33, 7717–7734, 2020.

Senior, C. and Ingram, W.: C02 and climate: A missing feedback, Nature, 341, 132–134, 1989.

Shell, K. M., Kiehl, J. T., and Shields, C. A.: Using the radiative kernel technique to calculate climate feedbacks in NCAR's Community Atmospheric Model, Journal of Climate, 21, 2269–2282, 2008.

Sherwood, S., Webb, M. J., Annan, J. D., Armour, K., Forster, P. M., Hargreaves, J. C., Hegerl, G., Klein, S. A., Marvel, K. D., Rohling, E. J., et al.: An assessment of Earth's climate sensitivity using multiple lines of evidence, Reviews of Geophysics, 58, e2019RG000 678, 2020.

Sherwood, S. C., Bony, S., and Dufresne, J.-L.: Spread in model climate sensitivity traced to atmospheric convective mixing, Nature, 505, 37–42, 2014.

Sherwood, S. C., Bony, S., Boucher, O., Bretherton, C., Forster, P. M., Gregory, J. M., and Stevens, B.: Adjustments in the forcing-feedback framework for understanding climate change, Bulletin of the American Meteorological Society, 96, 217–228, 2015.

Slingo, A.: A GCM parameterization for the shortwave radiative properties of water clouds, Journal of the Atmospheric Sciences, 46, 1419–1427, 1989.

Smith, C., Kramer, R., Myhre, G., Forster, P., Soden, B. J., Andrews, T., Boucher, O., Faluvegi, G., Fläschner, D., Hodnebrog, Ø., et al.: Understanding rapid adjustments to diverse forcing agents, Geophysical Research Letters, 45, 12–023, 2018.

Smith, C. J.: HadGEM2 Radiative Kernels, https://doi.org/10.5518/406, 2018.

Soden, B. J. and Held, I. M.: An assessment of climate feedbacks in coupled ocean–atmosphere models, Journal of climate, 19, 3354–3360, 2006.

https://doi.org/10.5194/gmd-2021-11
Preprint. Discussion started: 8 March 2021

Soden, B. J., Broccoli, A. J., and Hemler, R. S.: On the use of cloud forcing to estimate cloud feedback, Journal of climate, 17, 3661–3665, 2004.

Soden, B. J., Held, I. M., Colman, R., Shell, K. M., Kiehl, J. T., and Shields, C. A.: Quantifying climate feedbacks using radiative kernels, Journal of Climate, 21, 3504–3520, 2008.

Swart, N. C., Cole, J. N., Kharin, V. V., Lazare, M., Scinocca, J. F., Gillett, N. P., Anstey, J., Arora, V., Christian, J. R., Hanna, S., et al.: The Canadian Earth System Model version 5 (CanESM5. 0.3), Geoscientific Model Development, 12, 4823–4873, 2019.

Tan, I., Storelvmo, T., and Zelinka, M. D.: Observational constraints on mixed-phase clouds imply higher climate sensitivity, Science, 352, 224–227, 2016.

Taylor, K. E., Stouffer, R. J., and Meehl, G. A.: An overview of CMIP5 and the experiment design, Bulletin of the American Meteorological Society, 93, 485–498, 2012.

Van der Dussen, J., De Roode, S., Dal Gesso, S., and Siebesma, A.: An LES model study of the influence of the free tropospheric thermodynamic conditions on the stratocumulus response to a climate perturbation, Journal of Advances in Modeling Earth Systems, 7, 670–691, 2015.

Vial, J., Dufresne, J.-L., and Bony, S.: On the interpretation of inter-model spread in CMIP5 climate sensitivity estimates, Climate Dynamics, 41, 3339–3362, 2013.

von Salzen, K., Scinocca, J. F., McFarlane, N. A., Li, J., Cole, J. N., Plummer, D., Verseghy, D., Reader, M. C., Ma, X., Lazare, M., et al.: The Canadian fourth generation atmospheric global climate model (CanAM4). Part I: representation of physical processes, Atmosphere-Ocean, 51, 104–125, 2013.

Webb, M. J., Andrews, T., Bodas-Salcedo, A., Bony, S., Bretherton, C. S., Chadwick, R., Chepfer, H., Douville, H., Good, P., Kay, J. E., et al.: The cloud feedback model intercomparison project (CFMIP) contribution to CMIP6, Geoscientific Model Development, 2017, 359–384, 2017.

Wood, R. and Bretherton, C. S.: On the relationship between stratiform low cloud cover and lower-tropospheric stability, Journal of climate, 19, 6425–6432, 2006.

Zahariev, K., Christian, J. R., and Denman, K. L.: Preindustrial, historical, and fertilization simulations using a global ocean carbon model with new parameterizations of iron limitation, calcification, and N2 fixation, Progress in Oceanography, 77, 56–82, 2008.

Zelinka, M. D. and Hartmann, D. L.: Why is longwave cloud feedback positive?, Journal of Geophysical Research: Atmospheres, 115, 2010.

Zelinka, M. D., Klein, S. A., and Hartmann, D. L.: Computing and partitioning cloud feedbacks using cloud property histograms. Part I: Cloud radiative kernels, Journal of Climate, 25, 3715–3735, 2012a.

Zelinka, M. D., Klein, S. A., and Hartmann, D. L.: Computing and partitioning cloud feedbacks using cloud property histograms. Part II: Attribution to changes in cloud amount, altitude, and optical depth, Journal of Climate, 25, 3736–3754, 2012b.

Zelinka, M. D., Klein, S. A., Taylor, K. E., Andrews, T., Webb, M. J., Gregory, J. M., and Forster, P. M.: Contributions of different cloud types to feedbacks and rapid adjustments in CMIP5, Journal of Climate, 26, 5007–5027, 2013.

Zelinka, M. D., Zhou, C., and Klein, S. A.: Insights from a refined decomposition of cloud feedbacks, Geophysical Research Letters, 43, 9259–9269, 2016.

Zelinka, M. D., Grise, K. M., Klein, S. A., Zhou, C., DeAngelis, A. M., and Christensen, M. W.: Drivers of the low-cloud response to poleward jet shifts in the North Pacific in observations and models, Journal of Climate, 31, 7925–7947, 2018.

Zelinka, M. D., Myers, T. A., McCoy, D. T., Po-Chedley, S., Caldwell, P. M., Ceppi, P., Klein, S. A., and Taylor, K. E.: Causes of higher climate sensitivity in CMIP6 models, Geophysical Research Letters, 47, 2020.

https://doi.org/10.5194/gmd-2021-11
Preprint. Discussion started: 8 March 2021

Zhou, C., Zelinka, M. D., Dessler, A. E., and Klein, S. A.: The relationship between interannual and long-term cloud feedbacks, Geophysical Research Letters, 42, 10–463, 2015.

485 Zhou, C., Zelinka, M. D., and Klein, S. A.: Analyzing the dependence of global cloud feedback on the spatial pattern of sea surface temperature change with a G reen's function approach, Journal of Advances in Modeling Earth Systems, 9, 2174–2189, 2017.